

*Climate of the Past Discussions* is the access reviewed discussion forum of *Climate of the Past*

# Impacts of land surface properties and atmospheric CO<sub>2</sub> on the Last Glacial Maximum climate: a factor separation analysis

A.-J. Henrot<sup>1</sup>, L. François<sup>2</sup>, S. Brewer<sup>2,\*</sup>, and G. Munhoven<sup>1</sup>

<sup>1</sup>Laboratory of Atmospheric and Planetary Physics, University of Liège, Liège, Belgium

<sup>2</sup>Unité de Modélisation du Climat et des Cycles Biogéochimiques, University of Liège, Liège, Belgium

\* now at: Botany Department, University of Wyoming, Laramie, Wyoming, USA

Received: 29 October 2008 – Accepted: 29 October 2008 – Published: 8 January 2009

Correspondence to: A.-J. Henrot (alexandra.henrot@ulg.ac.be)

Published by Copernicus Publications on behalf of the European Geosciences Union.

CPD

5, 29–71, 2009

Land surface  
properties and CO<sub>2</sub> –  
effects on LGM  
climate

A.-J. Henrot et al.

Title Page

Abstract

Introduction

Conclusions

References

Tables

Figures

⏪

⏩

◀

▶

Back

Close

Full Screen / Esc

Printer-friendly Version

Interactive Discussion

## Abstract

Many sensitivity studies have been carried out, using simplified GCMs to test the climate response to Last Glacial Maximum boundary conditions. Here, instead of adding the forcings successively as in previous studies, we applied the separation method of Stein and Alpert (1993), in order to determine rigourously the different contributions of the boundary condition modifications, and isolate the pure contributions from the interactions among the forcings. We carried out a series of sensitivity experiments with the model of intermediate complexity Planet Simulator, investigating the contributions of the ice sheet expansion and elevation, the lowering of the atmospheric CO<sub>2</sub> and of the vegetation cover change on the LGM climate. The results clearly identify the ice cover forcing as the main contributor to the cooling of the Northern Hemisphere, and also to the tropical precipitation disruption, leading to the southward shift of the ITCZ, while the orographic forcing mainly contributes to the disruption of the atmospheric circulation in the Northern Hemisphere. The isolated vegetation contribution also induces strong cooling over the continents of the Northern Hemisphere, that is further sufficient to affect the tropical precipitation and reinforce the southwards shift of the ITCZ, when combined with the ice forcing. The combinations of the forcings generate many non linear interactions, that reinforce or weaken the pure contributions, depending on the climatic mechanism involved, but they are generally weaker than the pure contributions. Finally, the comparison between the LGM simulated climate and climatic reconstructions over Eurasia suggests that our results reproduce well the south-west to north-east temperature gradients over Eurasia.

## 1 Introduction

The Last Glacial Maximum (LGM), around 21 000 years before present (21 kBP) represents the largest climate change of the recent past. It is characterized by changes in several climate forcings, resulting from the expansion and the thickening of the ice

CPD

5, 29–71, 2009

## Land surface properties and CO<sub>2</sub> – effects on LGM climate

A.-J. Henrot et al.

Title Page

Abstract

Introduction

Conclusions

References

Tables

Figures

⏪

⏩

◀

▶

Back

Close

Full Screen / Esc

Printer-friendly Version

Interactive Discussion



5 sheets at high latitudes, the large reduction in the atmospheric CO<sub>2</sub> concentration, and the less dense vegetation cover. Several projects, using palaeoclimatic data, have reconstructed the surface conditions at the LGM, like CLIMAP (CLIMAP Project Members, 1976), or more recently MARGO (Kucera et al., 2005), making of the LGM one of the best documented period of the recent geological past.

10 As a result, the LGM has become the subject of numerous General Circulation Model (GCM) studies, in order to test the ability of the models to simulate a climate markedly different from the present, and to better understand the mechanisms that lead to abrupt climate changes. Many sensitivity studies have been carried out, using GCMs to test the climate response to various glacial boundary conditions (Broccoli and Manabe, 15 1987b; Hewitt and Mitchell, 1997; Ganopolski, 2003; Schneider von Deimling et al., 2006). Nevertheless, in the frame of sensitivity studies, the boundary condition forcings are generally applied in a sequential procedure, that consists of a successive addition of the forcings leading to the final LGM state. In that case, the response of the model to a particular change in boundary condition is determined by the comparison of the runs with and without that change, neglecting in the analysis the possible interactions between the forcings, that can take place and contribute to the final climate state. Stein and Alpert (1993) developed a rigorous method to carry out sensitivity studies, that separates the pure contributions of the forcings from the interactions resulting from their combination.

20 In our study, we applied the factor separation method to a LGM sensitivity study. We used the Planet Simulator, an Earth system Model of Intermediate Complexity (described in Sect. 2) to carry out a series of sixteen simulation experiments, where we have assessed the effects from differences in the vegetation cover, the ice-sheet cover, the orography and the effect of reduced atmospheric carbon dioxide between a pre-industrial state and the LGM. We reconstructed the vegetation distributions with the CARAIB dynamic vegetation model (described in Sect. 2). We then examined the response of surface temperature and precipitation to the different forcings and discuss the pure contribution of the four factors on the LGM climate, as well as the interactions

---

## Land surface properties and CO<sub>2</sub> – effects on LGM climate

A.-J. Henrot et al.

---

[Title Page](#)[Abstract](#)[Introduction](#)[Conclusions](#)[References](#)[Tables](#)[Figures](#)[◀](#)[▶](#)[◀](#)[▶](#)[Back](#)[Close](#)[Full Screen / Esc](#)[Printer-friendly Version](#)[Interactive Discussion](#)

among them. Finally, we evaluated our LGM results over Eurasia and Africa against LGM climate reconstruction produced by Wu et al. (2007).

## 2 Model setup

The Planet Simulator (Fraedrich et al., 2005), an EMIC (Earth system Model of Intermediate Complexity) is based on its central component, the spectral atmospheric GCM, with triangular truncation, PUMA-2, developed from the atmospheric model PUMA (Fraedrich et al., 1998). PUMA-2 solves the moist primitive equations, representing the conservation of momentum, mass and energy, on  $\sigma$  coordinates in the vertical. It also includes boundary layer, precipitation, interactive clouds and radiation parametrizations. The applied version operates at a resolution of T21 and on 10 vertical equally spaced  $\sigma$  levels. The atmospheric module is coupled to a 50-m-deep mixed-layer ocean, a thermodynamic sea-ice and a land surface and soil model. Sea surface temperatures are computed from the net atmospheric heat flux in the surface. The transport of heat by oceanic surface currents is represented by an additional source or sink of heat, varying monthly and spatially, that is prescribed within the mixed-layer and the sea-ice. Heat flux adjustments on each grid-cell are performed within a preindustrial experiment, in which sea surface temperatures and sea-ice distribution are prescribed, using the AMIP2 dataset (AMIP2, 2004). We used here the preindustrial heat flux adjustment for the full set of experiments. We did not consider any change in the oceanic circulation at the LGM. The land surface and soil models calculate the surface temperatures by a linearized energy balance and predict soil moisture with a simple bucket parameterization. The influence of vegetation is represented by background albedo and roughness length. Their annual distributions are prescribed, and only albedo is modified in the presence of snow on the grid-cell.

The distributions of surface albedo and roughness length were obtained from the CARAIB dynamic vegetation model (CARbon Assimilation In the Biosphere) (Warnant et al., 1994; Nemry et al., 1996; Laurent et al., 2008). CARAIB calculates the carbon

Title Page

Abstract

Introduction

Conclusions

References

Tables

Figures



Back

Close

Full Screen / Esc

Printer-friendly Version

Interactive Discussion



fluxes between the atmosphere and the terrestrial biosphere, estimates the evolution of carbon pools, and calculates the relative abundance of a series of plant types. Its different modules focus, respectively on the hydrological cycle, photosynthesis and stomatal regulation, carbon allocation and biomass growth, heterotrophic respiration and litter and soil carbon, and the distribution of the model plant types, as a function of productivity. Here we used a 15 Plant functional Types (PFTs) classification, described in Galy et al. (2008), and translated the model PFT assemblages into biomes to produce vegetation maps. The inputs of the model are meteorological variables, which can be taken from meteorological databases or be outputs from GCMs. LGM vegetation distributions produced with CARAIB, using outputs from several GCMs to force the model, have already been discussed (François et al., 1998, 1999; Otto et al., 2002; Cheddadi et al., 2006; Galy et al., 2008). We chose one of the most satisfying LGM vegetation distributions, discussed in Sect. 4.1, to force the Planet Simulator, instead of a direct data reconstruction, to avoid the use of data interpolation.

### 3 Experimental setup

We carried out a series of sensitivity experiments with the Planet Simulator, implementing the factor separation method of Stein and Alpert (1993). This approach calculates and isolates the pure contribution of any factor, as well as the contributions due to interactions among two or more factors, using a linear combination of a number of simulations.  $2^n$  simulations are then required to separate the pure and interaction contributions of  $n$  factors. Following the factor separation method, we carried out a series of sixteen sensitivity experiments, considering all the possible perturbations of a given control run configuration by prescribing changes of ice-sheet cover, orography, vegetation cover (through albedo and roughness length) and atmospheric carbon dioxide. Table 1 lists the changes in boundary conditions used for the sixteen experiments. The control experiment incorporates none of the changes, while the LGM experiment includes all of them. We included the LGM land-sea distribution and orbital forcing in

Title Page

Abstract

Introduction

Conclusions

References

Tables

Figures

◀

▶

◀

▶

Back

Close

Full Screen / Esc

Printer-friendly Version

Interactive Discussion

the control configuration, taking into account their contributions to produce a complete LGM climate at the end of the series, but neglecting the contribution of their interactions with the other factors, since they are relatively weak (Sect. 4.2). However we did not consider the oceanic contribution to the LGM climate, since the mixed-layer model does not modify the oceanic heat transfer.

### 3.1 Boundary conditions and model configuration

The experiments, including the CTRL run, use common orbital forcings, land-sea distribution and oceanic configuration. The orbital parameters correspond to 21kBP (eccentricity  $0.018994^\circ$ , longitude of perihelion  $114.42^\circ$  and obliquity  $22.949^\circ$ ). The solar constant is kept fixed at  $1365 \text{ W/m}^2$ . The model's land distribution takes into account the emergence of land points due to the lower sea-level at 21kBP. The land-sea mask has been reconstructed from Peltier's ICE-5G  $1^\circ$  by  $1^\circ$  resolution ice sheet reconstruction (Peltier, 2004), interpolated onto the model's grid. As oceanic initial conditions, we used preindustrial sea surface temperatures and sea-ice distributions, and we prescribed the heat transfer calculated by the Planet Simulator for a preindustrial climate, as oceanic boundary condition.

The CTRL experiment was forced using a preindustrial atmospheric  $\text{CO}_2$  concentration of 280 ppmv. The control continental ice cover and orography have been reconstructed from Peltier's ICE-5G for the preindustrial state, considering that grid-cells covered by an ice fraction higher than 50% are completely covered by ice (see Fig. 1). The vegetation parameters have been derived from a preindustrial vegetation distribution calculated from an equilibrium run of CARAIB, forced with 280 ppmv of  $\text{CO}_2$  and the climatology of the CLIMATE database version 2.1 (W. Cramer, Potsdam, personal communication). However, the emerging cells from the LGM land-sea distribution keep their oceanic albedo and roughness length, to avoid extrapolating the preindustrial vegetation on these extra land points.

To obtain the LGM climate, we lowered the atmospheric  $\text{CO}_2$  concentration to an ice age level of 200 ppmv (Petit et al., 1999). We reconstructed the continental ice cover

## Land surface properties and $\text{CO}_2$ – effects on LGM climate

A.-J. Henrot et al.

Title Page

Abstract

Introduction

Conclusions

References

Tables

Figures

⏪

⏩

◀

▶

Back

Close

Full Screen / Esc

Printer-friendly Version

Interactive Discussion



and orography from Peltier's ICE-5G for the LGM (see Fig. 1). The vegetation parameters have been replaced by their LGM distributions derived from a LGM vegetation distribution produced by CARAIB. We used an equilibrium run of CARAIB forced with 200 ppmv of CO<sub>2</sub> and a climate derived from the ECHAM4 GCM Roeckner et al., 1996 (revised version of the distribution shown by François et al., 2003). We calculated the anomalies of the GCM climatic fields between the LGM and the preindustrial, added to the Cramer and Leemans dataset, as climatic inputs for the LGM simulation, following the approach described in Otto et al. (2002).

## 4 Results

### 4.1 Simulated LGM vegetation

The biome maps (Fig. 2) show the simulated preindustrial and LGM vegetation distributions, with a resolution of 0.5° by 0.5°. Globally, the simulated LGM vegetation cover is less dense than the preindustrial one. Grasslands and deserts expand, mainly at the expense of forest ecosystems, a response to the extremely cold and dry LGM conditions. CARAIB simulates a reduction of the total carbon stock (vegetation plus soil) of 734 GtC, which is in the lower part of the LGM carbon stock reduction range suggested from reconstructions of palaeovegetation from palynological and sedimentological proxy data (−700 to −1600 GtC), but slightly higher than biospheric model (forced with outputs of general circulation models) estimations (0 to 700 GtC) (Pedersen et al., 2003).

Regionally, the simulated LGM vegetation distribution is broadly consistent with the results of the Palaeovegetation Mapping Project BIOME 6000<sup>1</sup> (Prentice and Jolly, 2000; Harrison et al., 2001; Bigelow et al., 2003; Pickett et al., 2004). Polar desert and tundra are modelled in a large part of the Northern Hemisphere continents. In

<sup>1</sup>available on [http://www.bridge.bris.ac.uk/resources/Databases/BIOMES\\_data](http://www.bridge.bris.ac.uk/resources/Databases/BIOMES_data)

Title Page

Abstract

Introduction

Conclusions

References

Tables

Figures

⏪

⏩

◀

▶

Back

Close

Full Screen / Esc

Printer-friendly Version

Interactive Discussion

---

**Land surface  
properties and CO<sub>2</sub> –  
effects on LGM  
climate**

---

A.-J. Henrot et al.

---

[Title Page](#)[Abstract](#)[Introduction](#)[Conclusions](#)[References](#)[Tables](#)[Figures](#)[⏪](#)[⏩](#)[◀](#)[▶](#)[Back](#)[Close](#)[Full Screen / Esc](#)[Printer-friendly Version](#)[Interactive Discussion](#)

Siberia and the part of Alaska not covered by ice sheets, they replace the boreal forests (taiga), when in Western Europe tundra replaces the temperate forests. Note that the polar desert or ice biome, extremely expanded in our LGM simulation, does not represent permanent ice, but the absence of vegetation, due to extremely cold and dry conditions. The warm temperate and mixed forests of Southwestern Europe are replaced by semi-deserts. Colder forest types also appear in our results, as in the reconstruction of Cheddadi et al. (2006), that differs from the BIOME 6000 results, reconstructing only semi-deserts in the region. North Africa is covered by deserts, with a southward expansion of the Sahara, by less than 5° in latitude, replacing tropical grasslands or savannas. In Equatorial Africa the tropical rainforest is reduced, except in the western part. In Asia, deserts and grasslands expand, with an extension of deserts to the east in the center of Asia, and the replacement of subtropical and temperate forests by tropical grasslands essentially in Southeastern Asia. In North America, the forest biomes are shifted southwards and replaced by tundra or polar deserts, and the subtropical types are limited to Florida. However, the predominance of deserts and grasslands in the west coast of North America, simulated by CARAIB, does not agree with the reconstructions of Williams et al. (2000) used in the BIOME 6000 results, which show mainly cool mixed forests and open woodlands in this region. It is more in line with the reconstruction of Adams et al. (1990). A fragmentation of the tropical rainforest and its replacement by savannas or subtropical forests occur in the north of South America, while the southern part is dominated by tundra and deserts. Finally, the tropical grasslands and deserts prevailing in the center and the southwest of Australia, in the simulated preindustrial distribution, are replaced by warm and open forests.

## 4.2 Control experiment

As mentioned before, the control state differs from a preindustrial one by the 21 kBP orbital configuration and land-sea distribution, that we separate from the other factors, due to the weak contributions of their interactions. Nevertheless, the pure effects of both factors contribute to the LGM climate. The orbital forcing cools the preindustrial

global mean surface temperature of 15.2°C by 0.4°C, but does not significantly affect the precipitation. Locally, the cooling does not exceed 0.5°C, but reaches -4°C over sea-ice, especially in the Antarctic ocean, due to the persistence of sea-ice in summer, following the lowering of the obliquity at 21kBP, which reduces insolation at high latitudes in both hemispheres during their respective summers. The modification of the land-sea mask (with emerging grid-cells keeping oceanic surface albedo) warms the global mean temperature by 0.3°C. This warming is mainly due to the replacement of ocean by land grid-cells, preventing the formation of sea-ice on some grid-cells at high latitudes and the resulting strong albedo feedback to take place, and limiting the evaporation on some emerged grid-cells in the tropics. Finally, the CTRL climate, combining both forcings, is close to a preindustrial climate (with a global surface temperature lowered by -0.1°C only). The surface temperature and precipitation distributions for the control state are shown in Fig. 3.

### 4.3 Global responses

We present here the global impacts of the pure contributions of the four factors, as well as the contributions of their interactions. The magnitude of the impacts of boundary condition changes on surface temperature and precipitation are shown in Fig. 4, representing the anomalies between each experiment and the control run. Ice cover change (experiment I) is the factor producing globally the largest cooling and dryness, followed by CO<sub>2</sub> (experiment C), which gives an additional cooling effect when added notably to the ice cover change (experiment CI). Vegetation cover changes also significantly cool and dry the climate (experiment V), when orography changes slightly tend to warm the global climate (experiment O). The experiment CIV, adding ice, CO<sub>2</sub> and vegetation changes, is then the coolest and the driest of the series, even more than the complete LGM one, due to the absence of orography change. The global LGM cooling is -5.2°C (-10.4°C on the continents and -1.8°C on the oceans), and the global LGM precipitation reduction is -79 mm/yr (-105 mm/yr on the continents and -45 mm/yr on the oceans). Our LGM cooling is in line with PMIP1 (Palaeoclimate Mod-

## Land surface properties and CO<sub>2</sub> – effects on LGM climate

A.-J. Henrot et al.

Title Page

Abstract

Introduction

Conclusions

References

Tables

Figures



Back

Close

Full Screen / Esc

Printer-friendly Version

Interactive Discussion



elling Intercomparison Project) atmospheric GCMs (AGCMs) simulated coolings (from  $-2$  to  $6^{\circ}\text{C}$  for computed sea surface temperatures) (Joussaume and Taylor, 2000), but nearer the upper end of the range, since we take into account the impact of vegetation cover change, that was not the case in the PMIP1 simulations. Our LGM cooling also compares well with the PMIP2 atmosphere-ocean coupled GCM (AOGCMs) coolings, between  $-3.6$  and  $-5.7^{\circ}\text{C}$  (Braconnot et al., 2007), even with the use of prescribed oceanic heat fluxes in the Planet Simulator.

Figure 5 shows the effects on global, continental and oceanic surface temperature and precipitation that are uniquely due to the interaction of two or more factors. The contributions of the pure factors (ice,  $\text{CO}_2$ , vegetation and orography anomalies) are shown here for comparison. Note that we do not consider Antarctica for the continental mean, since large changes especially in surface temperature can occur, with a weak impact on local climate and which are not indicative of large scale climate change. The interactions should be taken into account in the climate analysis, since they show evidence of the non linear feature of effects caused by the different factor combinations. For example, the combination of the ice and vegetation cover changes (experiment IV) produces non linear effects, that result in an increase of surface temperature and precipitation. These effects acts in the opposite direction of the pure contributions of ice and vegetation. The total cooling due to ice and vegetation cover changes ( $-3.8^{\circ}\text{C}$  on global surface temperature, see Fig. 4) is then weaker than the simple addition of both pure contributions ( $-2.7^{\circ}\text{C}$  for ice plus  $-1.3^{\circ}\text{C}$  for vegetation, that is  $-4^{\circ}\text{C}$ ), since the interaction between both forcings gives a slight warming (of  $+0.2^{\circ}\text{C}$  globally). Nevertheless, the interaction effects remain weaker than the pure contributions effects. Only the interactions between ice and vegetation, and ice and orography (experiments IV and IO) have comparable effects to the pure contribution ones, especially on the continents. The interaction IO notably warms the continental surface temperature by  $0.4^{\circ}\text{C}$ , while the pure orographic contribution leads to a continental warming of  $0.9^{\circ}\text{C}$ . The increase of precipitation caused by the interaction IV ( $+31$  mm/yr) also compares to the decrease of precipitation due to the  $\text{CO}_2$  contribution ( $-33$  mm/yr).

---

## Land surface properties and $\text{CO}_2$ – effects on LGM climate

A.-J. Henrot et al.

---

[Title Page](#)[Abstract](#)[Introduction](#)[Conclusions](#)[References](#)[Tables](#)[Figures](#)[⏪](#)[⏩](#)[◀](#)[▶](#)[Back](#)[Close](#)[Full Screen / Esc](#)[Printer-friendly Version](#)[Interactive Discussion](#)

## 4.4 Spatial responses

### 4.4.1 Surface temperature

Figures 6 and 7 illustrate the surface temperature responses, to the prescription of the boundary condition forcings. The presence of ice sheets increases the albedo of ice covered grid-cells by more than 40% in comparison to the control state. The pure ice cover effect (experiment I) produces the largest cooling only in the Northern Hemisphere, in comparison to the other pure contributions of the series, but weakly affects the Southern Hemisphere. The largest decreases of surface temperature are located over the ice sheets and over the North Atlantic and the Arctic Oceans, resulting from an extension and thickening of sea-ice. The mid and low northern latitudes are also affected by some weaker cooling, but some tropical regions, as Equatorial Africa and India, are subjected to warmings, more pronounced during summer and linked to a decrease of summer rainfall. The weak impact of the ice cover effect in the Southern Hemisphere is due to the lack of oceanic circulation changes in our model. Only the small ice cap covering Patagonia leads to a pronounced local cooling.

Vegetation cover changes result in a large cooling on the Northern Hemisphere, mainly over the continents (experiment V). The vegetation contribution is comparable in terms of magnitude to the ice cover effect over the mid and low latitudes of the Northern Hemisphere. As described above, vegetation cover changes affect surface albedo and roughness length, but the albedo impact on surface temperature is dominant, because of its direct impact on the energy balance. The cooling produced on the continents of the Northern Hemisphere is directly linked to the increase of surface albedo by more than 10%, caused by the replacement of boreal and temperate forests by tundra or semi-deserts. Further, the cooling induced can be reinforced by the snow albedo feedback, on grid-cells covered by snow. However, Equatorial Africa and India also show some warming, related to a decrease of evaporation and summer rainfall, as in experiment I. Surface temperatures also increase in Australia and South Africa, but are caused instead by the increase of surface albedo, caused by the replacement

Title Page

Abstract

Introduction

Conclusions

References

Tables

Figures



Back

Close

Full Screen / Esc

Printer-friendly Version

Interactive Discussion

---

**Land surface  
properties and CO<sub>2</sub> –  
effects on LGM  
climate**

---

A.-J. Henrot et al.

---

[Title Page](#)[Abstract](#)[Introduction](#)[Conclusions](#)[References](#)[Tables](#)[Figures](#)[⏪](#)[⏩](#)[◀](#)[▶](#)[Back](#)[Close](#)[Full Screen / Esc](#)[Printer-friendly Version](#)[Interactive Discussion](#)

of deserts and grasslands by forest biomes. Finally, there is pronounced but localized cooling over emerging land grid-cells at LGM, due to the replacement of their control oceanic albedos of 7% directly by LGM vegetation albedo greater than 15%. In experiment IV, the application of vegetation changes together with the presence of ice sheets reinforces and expands southwards the cooling induced by the ice cover effect, especially over the high latitudes and the continents in the Northern Hemisphere. A stronger warming occur in Equatorial Africa and India. However, the Southern Hemisphere remains weakly affected by both factors. Only vegetation changes produce a weak warming, due to a decrease in albedo.

The CO<sub>2</sub> contribution causes a rather uniform temperature cooling, of about  $-2^{\circ}\text{C}$  (experiment C). The magnitude of the cooling is similar over continents and oceans, and in both Northern and Southern Hemispheres, making it the most important contributor to sea surface temperature cooling. Further, the CO<sub>2</sub> contribution results in a stronger cooling around the poles, especially over the Antarctic ocean, linked to an expansion and thickening of sea-ice. This reinforces the cooling trend in the Northern Hemisphere initiated by ice sheet and vegetation albedo effects, when all three forcings are combined (experiment CIV), and gives an additional cooling in the Southern Hemisphere, notably stronger than the vegetation warming impact in Australia and South Africa.

In contrast to the previous contributions, orography changes do not have a net cooling effect in the Northern Hemisphere (experiment O). The increased elevation produces large cooling over the ice sheets, especially over the Laurentide ice sheet, which has its surface at 3000 m a.s.l. in the LGM reconstruction. The cooling also affects the Arctic and North Atlantic oceans. However, North America, Europe, and also North West Pacific and North Atlantic experiment large warmings linked to precipitation changes, caused by wind track perturbations at mid and high latitudes, as discussed below. The combination of the ice sheet cover and orography forcings, representing the full contribution of the ice sheets on surface temperature of the ice sheets at LGM, leads to an additional cooling over the ice sheets. The cooling is weaker over the southern

---

**Land surface  
properties and CO<sub>2</sub> –  
effects on LGM  
climate**

---

A.-J. Henrot et al.

borders of the ice sheets, due to the orographic contribution. The cooling trend induced by ice cover then remains dominant over the continents of the Northern Hemisphere, when the orography changes minimizes the cooling at the mid latitudes and slightly warms some oceanic regions, e.g. North West Pacific and Southern Oceans, where the ice albedo has weaker impacts.

The combination of the four factors (experiment LGM), keeps the cooling profile induced by ice cover, vegetation and CO<sub>2</sub> changes, as in the experiment CIV. However, experiment LGM is warmer than experiment CIV, due to the contribution of orography changes, warming the oceans and some continental regions of the mid latitudes in the Northern Hemisphere.

#### 4.4.2 Precipitation

Figures 8 and 9 illustrate the significative precipitation responses to the prescribed boundary condition forcings. In experiment I, the cooling induced by ice cover effect dries out the atmosphere, and reduces precipitation. Large reductions occur in the Northern Hemisphere, over the ice sheets, Siberia, Alaska and the North Atlantic Ocean. Further, the intense cooling of the continents strengthens the westerlies of the Northern Hemisphere, giving rise to precipitation in North America and North Pacific. Nevertheless, the impact of ice cover is not limited to the high latitudes and also strongly influences the tropical precipitation system by a southward shift of the control location of the Inter Tropical Convergence Zone (ITCZ). The strong cooling impact of ice cover on the surface and sea surface temperature in the Northern Hemisphere causes an increase of the inter-hemispheric temperature gradient, sufficient to lead to a displacement of the ITCZ to the warmer Southern Hemisphere. This explains the reduction of precipitation over the oceans and the continent and the weakening of the monsoon systems (except over southeastern China) in the northern part of the tropics (ITCZ control location), and the increase of precipitation to the south.

Vegetation changes in experiment V in turn dry out the continents of the Northern Hemisphere, mainly due to the cooling effect of the increase of albedo. The cooling ef-

[Title Page](#)[Abstract](#)[Introduction](#)[Conclusions](#)[References](#)[Tables](#)[Figures](#)[⏪](#)[⏩](#)[◀](#)[▶](#)[Back](#)[Close](#)[Full Screen / Esc](#)[Printer-friendly Version](#)[Interactive Discussion](#)

---

**Land surface  
properties and CO<sub>2</sub> –  
effects on LGM  
climate**

---

A.-J. Henrot et al.

[Title Page](#)[Abstract](#)[Introduction](#)[Conclusions](#)[References](#)[Tables](#)[Figures](#)[⏪](#)[⏩](#)[◀](#)[▶](#)[Back](#)[Close](#)[Full Screen / Esc](#)[Printer-friendly Version](#)[Interactive Discussion](#)

fect again strengthens the westerlies, increasing precipitation over the center of North America, and is similar, but weaker in magnitude, to the ice cover effect. The tropics also undergo a strong reduction of precipitation, as in experiment I. By the same mechanism, the contribution of the vegetation changes is then sufficient to shift the ITCZ location southwards, then reducing oceanic and continental precipitation in the northern part of the tropics. Nevertheless, the reduction of the rainforest in Amazonia, Equatorial Africa or Indonesia could also be responsible for the reduction of precipitation over these regions. The change of vegetation from rainforest to grasslands or savannas decreases the roughness length, that in turn decreases the surface evaporation, thus warming and drying the air. The change in precipitation could be linked to the roughness length more than to the albedo effect. The combination of vegetation changes with ice cover reinforces the dryness induced by ice albedo in the Northern Hemisphere, and intensifies the ITCZ shift, further decreasing rainfall over the ITCZ control location and increasing them southwards.

Orography changes strongly affect precipitation over the mid and high latitudes of the Northern Hemisphere, by disrupting the atmospheric circulation. The presence of the high Laurentide ice sheet causes a split flow of the westerlies into two branches, one passing northwards of the ice sheet and the other southwards, and rejoining over the North Atlantic. As we can see on Fig. 10, showing the surface winter winds for the experiments CTRL and O, the split flow causes at the surface a deflection of the westerlies over Alaska and the formation of an anticyclonic circulation over the western portion of the Laurentide ice sheet. The northern part of the ice sheet is then crossed by a strong surface flow, which increases precipitation there, while the southern part and the rest of North America is crossed by north to northwest flow originating from the anticyclone, which causes a decrease of rainfall in these region. These conditions prevail during winter, spring and autumn, but weaken during summer. Over the North Atlantic, where both flows merge together, precipitation generally increases. The deflection of the westerly wind belt over the North Atlantic, with south to southwest winds arriving to the southern part of the Fennoscandian ice sheet, increases precipitation

---

**Land surface  
properties and CO<sub>2</sub> –  
effects on LGM  
climate**

---

A.-J. Henrot et al.

---

[Title Page](#)[Abstract](#)[Introduction](#)[Conclusions](#)[References](#)[Tables](#)[Figures](#)[⏪](#)[⏩](#)[◀](#)[▶](#)[Back](#)[Close](#)[Full Screen / Esc](#)[Printer-friendly Version](#)[Interactive Discussion](#)

on the ocean. However, it decreases the wind strength over Western Europe, causing a large reduction of precipitation in the main part of Eurasia, explaining the net warming of the surface temperature described above. The Fennoscandian ice sheet also blocks the westerlies, which contributes to the decrease of precipitation over Eurasia. The total ice sheet contribution, combining ice cover and orography forcings (experiment IO), keeps the precipitation profile imposed by orography changes in the Northern Hemisphere, and imposed by the ice albedo in the tropics. Nevertheless, the ice albedo cooling effect tends to increase the dryness of the continents of the Northern Hemisphere, except over North America, where the intensification of the westerlies causes more precipitation. The shift of the ITCZ over the ocean is more pronounced, which can be linked to the further increase of the surface temperature gradient, due to warmer sea surface temperatures in the south, induced by orography changes.

The CO<sub>2</sub> contribution has the weakest impact on precipitation in the Northern Hemisphere, and dries out equally both hemispheres. Only the equatorial band is affected by a more pronounced decrease of precipitation, still weaker than the other pure contributions, that can be related to the CO<sub>2</sub> induced sea surface temperature cooling. The combination of the CO<sub>2</sub> effect with the ice cover and vegetation change effects, generates the driest experiment of the series (experiment CIV), causing strong reductions of precipitation over the continents and a pronounced southward shift of the ITCZ. The addition of the orography contribution, in the experiment LGM, essentially modifies the precipitation distributions in the Northern Hemisphere, generating more precipitation over the north and north-west of the Laurentide ice sheet, in comparison to the experiment CIV. However, the drying over the continents of the Northern Hemisphere is reinforced, as well as the decrease of rainfall over the ITCZ control location.

#### 4.4.3 Interaction effects

The global effect of the interactions among factors generally tend to increase temperatures and precipitation. However, the interactions have much more contrasted local effects, that may weaken or reinforce the pure contribution effects, depending on the

region. We discuss here only the strongest interactions of the series, which are the interactions between ice cover and vegetation change (IV), and between ice cover and orography changes (IO), respectively. The other interactions of the series (OV, IOV, etc.) show similar patterns in their effects, but are weaker. We can also remark that the interactions between CO<sub>2</sub> changes and the other factors generates the weakest effects of the series. Figure 11 shows the effects on surface temperature and precipitation of the interactions IV and IO.

Both interactions IV and IO warm the surface temperature over sea-ice in the Arctic Ocean, with the interaction IO causing a greater warming, even affecting the northern borders of the continents. The interactions here weaken the pure contributions of the three factors, that tend to increase the sea-ice extent and thickness in the Arctic, avoiding the regional climate to cool intensively. In contrast, in the Antarctic Ocean, the interactions favor the sea-ice extent and thickening.

The interaction IV produces strong continental coolings, comparable in magnitude to the pure contributions, e.g. in Alaska. The increase of surface albedo due to both contributions, cools the surface temperature, allowing snow to persist and the positive snow albedo feedback to reinforce the initial cooling induced by both pure contributions. However, over Equatorial Africa and India, the interaction leads to a cooling together with a precipitation increase. These effects can be related to a more important surface evaporation, permitted by the decrease of the sensible heat flux, due to the southward extension of the cooling trend caused by both I and V forcings. In this case, the interaction acts in the opposite direction of both pure contributions, and lower their regional warming impacts.

The interaction IO produces strong coolings over the continents, particularly over North America, with an increase of rainfall. The interaction effect is opposite to the orographic warming effect in the concerned region. This regional cooling can be related to the ice induced cooling, reinforced by the snow albedo feedback, and possibly to the local topographic cooling induced by the orography change. However, precipitation also increases, related to the combined effects of the strengthening of the winds due to the

---

## Land surface properties and CO<sub>2</sub> – effects on LGM climate

A.-J. Henrot et al.

---

[Title Page](#)[Abstract](#)[Introduction](#)[Conclusions](#)[References](#)[Tables](#)[Figures](#)[Back](#)[Close](#)[Full Screen / Esc](#)[Printer-friendly Version](#)[Interactive Discussion](#)

ice contribution and the intensification of the northern branch of the jet stream due to the orography contribution. However, the interaction IO mainly affects the precipitation in the Northern Hemisphere, while the interaction IV essentially concerns the tropics.

## 5 Discussion

### 5.1 Boundary condition forcings

The complete series of experiments allows us to analyse and distinguish several climatic impacts on the LGM climate, linked to the development of ice sheets, the lowering of atmospheric CO<sub>2</sub> and vegetation changes. The factor separation method used here allows us to compare the relative roles of the factors, starting from the same control state. The procedure differs from previous sensitivity studies that already pointed out the same glacial forcings at LGM, but added them successively (Broccoli and Manabe, 1987b; Hewitt and Mitchell, 1997; Ganopolski, 2003; Schneider von Deimling et al., 2006). The method used here also avoids a threshold effect, that could be reached when the forcings are added successively, each forcing modifying the climate state of the model. In consequence, the magnitude of an effect can depend on the order in which the forcings are applied. Further, we are able to isolate the climatic effects resulting from the interactions between different factors. The disadvantage of this method is that it requires a large number of experiments to be carried out, which can be minimized by a rigorous choice of the forcing studied. It is also best suited for use with an EMIC, to further reduce the time requirement of the study.

Our results compare well with the results of previous sensitivity studies mentioned above. The order of magnitude of the pure contributions is notably in line with the results of CLIMBER (Ganopolski, 2003), that already showed the dominant cooling effect of the ice sheets (ice plus orography) ( $-3^{\circ}\text{C}$  globally), followed by the lowering of CO<sub>2</sub> ( $-1.2^{\circ}\text{C}$ ) and finally vegetation cover changes ( $-0.7^{\circ}\text{C}$ ). However, the vegetation contribution we obtain is much more pronounced than the one obtained in previous

Title Page

Abstract

Introduction

Conclusions

References

Tables

Figures

⏪

⏩

◀

▶

Back

Close

Full Screen / Esc

Printer-friendly Version

Interactive Discussion

sensitivity studies with uncoupled vegetation model (Ganopolski, 2003; Crowley and Baum, 1997; Kubatzki and Claussen, 1998; Levis et al., 1999; Wyputta and McAveney, 2001; Crucifix and Hewitt, 2005). This results from the rigorous separation of the factor impacts, fully isolating the vegetation contribution from the effects of the other contributions and of their interactions.

The separation of the ice cover and orography contributions shows that the ice albedo effect is the main contributor to the cooling of the Northern Hemisphere, when orography has only a local cooling impact over the ice sheet. Several studies have already investigated both effects, but in a sequentially additive procedure (Rind, 1987; Kageyama and Valdes, 2000). The isolation of both contributions allows us to attribute the atmospheric circulation changes in the Northern Hemisphere to the orography effect, but the strengthening of the westerlies of the Northern Hemisphere to the ice albedo effect. As in Manabe and Broccoli (1985) and Broccoli and Manabe (1987a), the presence of the Laurentide ice sheet has a predominant impact on the atmospheric circulation, causing a split flow of the westerlies into two branches, that in turn leads to a disruption of the precipitation distributions in the Northern Hemisphere, and affects the surface temperature. We can also remark that the orographic contribution alone would have caused some warming in Europe and the center of North America. These warmings are finally overpassed by the cooling effect of the ice cover, but the resulting impact of the ice sheets (orography plus ice albedo) in these regions is weaker than the pure ice albedo effect.

Nevertheless, the ice sheet impact is not limited to the Northern Hemisphere, since the ice cover contribution significantly affects the tropical regions, and is even the main contributor to tropical precipitation decrease over the continents and the oceans. Chiang et al. (2003), Chiang and Bitz (2005), and Broccoli et al. (2006) already related the presence of ice in the Northern Hemisphere to the reduction of convective activity and precipitation in the tropics and particularly to the southwards shift of the ITCZ (Braconnot et al., 2000). In our case, the pure contribution of the ice sheet cover is sufficient to produce a reduction of the sea surface temperature in the Northern Hemisphere

---

## Land surface properties and CO<sub>2</sub> – effects on LGM climate

A.-J. Henrot et al.

---

[Title Page](#)[Abstract](#)[Introduction](#)[Conclusions](#)[References](#)[Tables](#)[Figures](#)[Back](#)[Close](#)[Full Screen / Esc](#)[Printer-friendly Version](#)[Interactive Discussion](#)

---

**Land surface  
properties and CO<sub>2</sub> –  
effects on LGM  
climate**

---

A.-J. Henrot et al.

[Title Page](#)[Abstract](#)[Introduction](#)[Conclusions](#)[References](#)[Tables](#)[Figures](#)[⏪](#)[⏩](#)[◀](#)[▶](#)[Back](#)[Close](#)[Full Screen / Esc](#)[Printer-friendly Version](#)[Interactive Discussion](#)

its local contribution, especially on the continents in the Northern Hemisphere, is the weakest of the four pure contributions. Further, CO<sub>2</sub> induces very weak non linear interactions with the other factors, and always tends to reinforce the cooling and the drying induced by the other factors.

## 5 5.2 Consistency with palaeo data

In order to estimate the consistency of the simulated LGM climate and of the boundary conditions impacts, we evaluated our results over Eurasia and Africa against the LGM climate reconstructed by Wu et al. (2007). We have only compared continental climate, to limit the oceanic influence, since our model does not include an OGCM. The Wu et al. (2007) reconstruction was produced with an improved inverse vegetation model, using a recent version of BIOME 4 (Kaplan, 2001) and pollen biome scores from the BIOME 6000 project (Prentice and Jolly, 2000). Further, the improved inverse modelling method takes into account the direct physiological impact of the lower CO<sub>2</sub> concentration at LGM, reducing the bias in palaeoclimatic reconstruction (Ramstein et al., 2007).

We compare our model results to reconstructions through zonal averages in the longitudinal direction, following the approach of Kageyama et al. (2001). We have chosen two sectors representing Western Europe and Africa (20° W–20° E) and Eastern Europe, Eastern Africa and Western Siberia (20° E–60° E). The average are taken over land points only. Figures 12 and 13 show the zonal averages of the model anomalies and the data anomalies between LGM and modern climate for the MTCO (mean temperature of the coldest month), MTWA (mean temperature of the warmest month), MAT and MAP (respectively mean annual temperature and precipitation). We also add the data error bars, representing the 5–95% confidence interval for each reconstruction and the ±2 standard deviation curves, representing the longitudinal dispersion of the model results. Note that the anomalies are calculated between a modern climate run (same conditions as for preindustrial except a CO<sub>2</sub> concentration of 340 ppmv) and the LGM run, in order to be compatible with the reconstructed anomalies.

## Land surface properties and CO<sub>2</sub> – effects on LGM climate

A.-J. Henrot et al.

Title Page

Abstract

Introduction

Conclusions

References

Tables

Figures

⏪

⏩

◀

▶

Back

Close

Full Screen / Esc

Printer-friendly Version

Interactive Discussion



---

**Land surface  
properties and CO<sub>2</sub> –  
effects on LGM  
climate**

---

A.-J. Henrot et al.

[Title Page](#)[Abstract](#)[Introduction](#)[Conclusions](#)[References](#)[Tables](#)[Figures](#)[⏪](#)[⏩](#)[◀](#)[▶](#)[Back](#)[Close](#)[Full Screen / Esc](#)[Printer-friendly Version](#)[Interactive Discussion](#)

where discrepancies remain significant. The model tends to overestimate the MTCO cooling and the dryness over Siberia, similar to several models in the PMIP1 project (Kageyama et al., 2001). This is mainly linked in our model to the extra cool and dry climate resulting from the presence of the ice cover in the Northern Hemisphere. As explained in Kageyama et al. (2001), it also may be due to the perturbation of atmospheric circulation produced by North Atlantic sea surface temperatures and sea-ice extent, computed by the slab ocean model. However the simulated sea surface temperatures do not produce in our model a less pronounced cooling over Western Europe than over the eastern part, that should also result from the atmospheric perturbation, and the MTCO cooling over Western Europe agree quite well with the data. On the other hand, the MTWA cooling is underestimated over Western Europe (around 45° N), linked to a decrease of MAP. These results may be related to too warm sea surface temperature computed by the slab model in the Mediterranean Sea, influencing the continental temperature and precipitation of this region, and giving warmer and drier summer than in the reconstruction. The weakening of the westerlies due to orography changes (see Sect. 4.4) can also explain the warming of the region. We can not really consider the low resolution of the model and the poor representation of orography in this region as mainly responsible for the discrepancies with the data, since Jost et al. (2005) have found that the discrepancies remained at higher resolutions.

Over Eastern and South Africa, the model systematically underestimates the MTCO and MTWA coolings. This underestimation of the cooling by the model can be explained by the higher elevation of the data points (above 1500 m), in comparison to the model elevation (not exceeding 500 m). The reduction of the reconstructed temperature are then larger at higher elevation, as suggested by the reconstruction of temperature changes at the LGM from the snowline changes in East Africa carried out by Mark et al. (2005).

---

**Land surface properties and CO<sub>2</sub> – effects on LGM climate**A.-J. Henrot et al.

---

[Title Page](#)[Abstract](#)[Introduction](#)[Conclusions](#)[References](#)[Tables](#)[Figures](#)[Back](#)[Close](#)[Full Screen / Esc](#)[Printer-friendly Version](#)[Interactive Discussion](#)

## 6 Conclusions

In this study, we used the model of intermediate complexity Planet Simulator to investigate the contributions of the ice sheet expansion and elevation, the lowering of the atmospheric CO<sub>2</sub> and of the vegetation cover change on the LGM climate. The vegetation distributions for the preindustrial and the LGM were produced by the dynamic vegetation model CARAIB. They compare fairly well in terms of biomes with the results of the Palaeovegetation Mapping Project BIOME 6000 (Prentice and Jolly, 2000).

Although previous studies already pointed out the role of the mentioned forcings on the LGM climate, we applied here the factor separation method of Stein and Alpert (1993), in order to determine rigorously the different contributions of the boundary condition modifications. The method also allows us to isolate the pure contributions, as well as the interactions among the factors.

According to Ganopolski (2003), on a global basis, the ice sheet expansion, towards mainly the ice albedo effect, is the main contributor of the cooling and drying of the LGM climate, followed by the lower CO<sub>2</sub> and then the vegetation cover change. The ice albedo effect is also responsible for the strongest cooling in the Northern Hemisphere, when the CO<sub>2</sub> lowering is the main contributor to the Southern Hemisphere cooling, as in Broccoli and Manabe (1987b).

The separation of the ice cover and orographic contributions clearly identifies the ice cover expansion in the Northern Hemisphere for being responsible for the tropical precipitation disruption, and the southward shift of the ITCZ, as already mentioned in (Chiang et al., 2003). The orographic changes mainly contribute to the disruption of the atmospheric circulation in the Northern Hemisphere, leading to a redistribution of the precipitation, without a significant impact on the tropics. The orographic contribution is even responsible for warmings on the continents of the Northern Hemisphere and on the oceans, that are at term overpassed by the cooling effect of the ice cover.

In our experiment, the vegetation contribution induces strong cooling over the continents of the Northern Hemisphere, mainly caused by the increase of albedo, even

Title Page

Abstract

Introduction

Conclusions

References

Tables

Figures



Back

Close

Full Screen / Esc

Printer-friendly Version

Interactive Discussion

comparable in magnitude to the ice cover induced coolings in some regions. The isolation of the vegetation contribution from the other ones lead to stronger impacts than in previous sensitivity studies (Crowley and Baum, 1997; Wyputta and McAveney, 2001). Further, the vegetation effects are also sufficient to affect the tropical precipitation on land, and on the oceans, causing a southward shift of the ITCZ, reinforced when we combine the ice and vegetation contributions.

The combinations of the factors generate many interactions, globally opposed to the pure contributions and weaker. However, locally the interaction effects are more complex and reinforce or weaken the pure contributions, depending on the regions of the globe and on the climatic mechanism involved.

Our LGM climate results agree fairly well with the climatic reconstructions of Wu et al. (2007) over Europe and Western Siberia, notably due to the inclusion of vegetation changes. Our results reproduce well the south-west to north-east temperature gradient decreasing MTCO from Europe to Siberia, and the absence of significant MTWA gradient, as in the PMIP1 and PMIP2 model-pollen data comparisons carried out by Kageyama et al. (2001, 2006). However, the model results underestimate the MTWA cooling over Western Europe, due to the lack of an interactive ocean, as well as the coolings over Africa, due to the use of elevated data points.

*Acknowledgements.* A.-J. Henrot is a Research Fellow and G. Munhoven a Research Associate with the Belgian Fund for Scientific Research (F.R.S.-FNRS).

## References

- Adams, J. M., Faure, H., Faure-Denard, L., McGlade, J. M., and Woodward, F. I.: Increases in the terrestrial carbon storage from the Last Glacial Maximum to the present, *Nature*, 348, 711–714, 1990. 36
- AMIP2: The second phase of the Atmospheric Model Intercomparison Project (AMIP2), Workshop WCRP/WGNE, Météo France, Toulouse, France, 2004. 32
- Bigelow, N. H., Brubaker, L. B., Edwards, M. E., Harrison, S. P., Prentice, I. C., Anderson, P. M., Andreev, A. A., Bartlein, P. J., Christensen, T. R., Cramer, W., Kaplan, J. O., Lozhkin, A. V.,

## Land surface properties and CO<sub>2</sub> – effects on LGM climate

A.-J. Henrot et al.

Title Page

Abstract

Introduction

Conclusions

References

Tables

Figures



Back

Close

Full Screen / Esc

Printer-friendly Version

Interactive Discussion



---

**Land surface  
properties and CO<sub>2</sub> –  
effects on LGM  
climate**A.-J. Henrot et al.

---

[Title Page](#)[Abstract](#)[Introduction](#)[Conclusions](#)[References](#)[Tables](#)[Figures](#)[⏪](#)[⏩](#)[◀](#)[▶](#)[Back](#)[Close](#)[Full Screen / Esc](#)[Printer-friendly Version](#)[Interactive Discussion](#)

Matveyeva, N. V., Murray, D. V., McGuire, A. D., Razzhivin, V. Y., Ritchie, J. C., Smith, B., Walker, D. A., Gajewski, K., Wolf, V., Holmqvist, B. H., Igarashi, Y., Kremenetskii, K., Paus, A., Pisaric, M. F. J., and Vokova, V. S.: Climate change and Arctic ecosystems I. Vegetation changes north of 55° N between the last glacial maximum, mid-Holocene and present, J. Geophys. Res., 108, 8170, 2003. 35

Braconnot, P., de Noblet, S. J. N., and Ramstein, G.: Mid-Holocene and Last Glacial Maximum African monsoon changes as simulated within the Paleoclimate Modelling Intercomparison Project, Global Planet. Change, 26, 51–66, 2000. 46

Braconnot, P., Otto-Bliesner, B., Harrison, S., Jousseaume, S., Peterchmitt, J.-Y., Abe-Ouchi, A., Crucifix, M., Driesschaert, E., Fichetef, T., Hewitt, C., Kageyama, M., and Kitoh, A.: Results of PMIP2 coupled simulations of the Mid-Holocene and Last Glacial Maximum – Part 1: experiments and large scale features, Clim. Past, 3, 261–277, 2007, <http://www.clim-past.net/3/261/2007/>. 38

Broccoli, A. J. and Manabe, S.: The effects of the Laurentide ice sheet on north american climate during the last glacial maximum, Géographie physique et Quaternaire, 41, 291–299, 1987a. 46

Broccoli, A. J. and Manabe, S.: The influence of continental ice, atmospheric CO<sub>2</sub>, and land albedo on the climate of the last glacial maximum, Climate Dyn., 1, 87–99, 1987b. 31, 45, 47, 51

Broccoli, A. J., Dahl, K. A., and Stouffer, R. J.: The response of the ITCZ to Northern Hemisphere cooling, Geophys. Res. Lett., 33, L01 702, 2006. 46

Cheddadi, R., Vendramin, G., Litt, T., François, L., Kageyama, M., Lorentz, S., Laurent, J., de Beaulieu, J., Sadori, L., Jost, A., and Lunt, D.: Imprints of glacial refugia in the modern genetic diversity of *Pinus sylvestris*, Global Ecology and Biogeography, 15, 271–282, 2006. 33, 36

Chiang, J. C. H. and Bitz, C. M.: Influence of high latitude ice cover on the marine Intertropical Convergence Zone, Climate Dyn., 25, 477–496, 2005. 46

Chiang, J. C. H., Biasutti, M., and Battisti, D. S.: Sensitivity of the Atlantic Intertropical Convergence Zone to Last Glacial Maximum boundary conditions, Paleoceanography, 18, 1094, 2003. 46, 51

CLIMAP Project Members: The Surface of the Ice-Age Earth, Science, 191, 1131–1137, 1976. 31

Crowley, T. J. and Baum, S. K.: Effect of vegetation on an ice-age climate model simulation, J.

---

**Land surface  
properties and CO<sub>2</sub> –  
effects on LGM  
climate**

---

A.-J. Henrot et al.

[Title Page](#)[Abstract](#)[Introduction](#)[Conclusions](#)[References](#)[Tables](#)[Figures](#)[⏪](#)[⏩](#)[◀](#)[▶](#)[Back](#)[Close](#)[Full Screen / Esc](#)[Printer-friendly Version](#)[Interactive Discussion](#)

Geophys. Res., 102, 16 463–16 480, 1997. 46, 52

Crucifix, M. and Hewitt, C. D.: Impact of vegetation changes on the dynamics of the atmosphere at the Last Glacial Maximum, *Climate Dyn.*, 25, 447–459, 2005. 46, 47

DeMenocal, P. B. and Rind, D.: Sensitivity of Asian and African Climate to Variations in Seasonal Insolation, Glacial Ice Cover, Sea Surface Temperature, and Asian Orography, *J. Geophys. Res.*, 98, 7265–7287, 1993. 47

Fraedrich, K., Kirk, E., and Lunkeit, F.: PUMA Portable University Model of the Atmosphere, Tech. Rep. 16, Meteorologisches Institut, Universität Hamburg, Hamburg, <http://www.mad.zmaw.de/fileadmin/extern/documents/reports/ReportNo.16.pdf>, 1998. 32

Fraedrich, K., Jansen, H., Kirk, E., Luksch, U., and Lunkeit, F.: The Planet Simulator: Towards a user friendly model, *Meteorol. Z.*, 14, 299–304, doi:10.1127/0941-2948/2005/0043, 2005. 32

François, L., Lorenz, S., M.Ghislain, Cheddadi, R., and Jolly, D.: Impact of reduced tropical sea surface temperatures on the reconstruction of climate and land vegetation at the last glacial maximum, in: *Proceedings XVI INQUA Congress*, p. 130, 2003. 35

François, L. M., Delire, C., Warnant, P., and Munhoven, G.: Modelling the Glacial-Interglacial Changes in the Continental Biosphere, *Global Planet. Change*, 16-17, 37–52, doi:10.1016/S0921-8181(98)00005-8, 1998. 33

François, L. M., Goddérís, Y., Warnant, P., Ramstein, G., de Noblet, N., and Lorenz, S.: Carbon stocks and isotopic budgets of the terrestrial biosphere at mid-Holocene and last glacial maximum times, *Chem. Geol.*, 159, 163–189, doi:10.1016/S0009-2541(99)00039-X, 1999. 33

Galy, V., François, L., France-Lanord, C., Faure, P., Kudrass, H., Palhol, F., and Singh, S. K.: C4 plants decline in the Himalayan basin since the Last Glacial Maximum, *Quaternary Sci. Rev.*, 27, 1396–1409, 2008. 33

Ganopolski, A.: Glacial integrative modelling, *Phil. Trans. R. Soc. Lond. Ser. A*, 361, 1871–1884, 2003. 31, 45, 46, 47, 51

Harrison, S. P., Yu, P., Takahara, H., and Prentice, I. C.: Paleovegetation – Diversity of temperate plants in east Asia, *Nature*, 413, 129–130, 2001. 35

Hewitt, C. D. and Mitchell, J. F. B.: Radiative forcing and response of a GCM to ice age boundary conditions: cloud feedback and climate sensitivity, *Climate Dyn.*, 13, 821–834, 1997. 31, 45

Jost, A., Lunt, D., Kageyama, M., Abe-Ouchi, A., Peyron, O., Valdes, P. J., and Ramstein, G.: High-resolution simulations of the last glacial maximum climate over Europe: a solution to

- discrepancies with continental palaeoclimatic reconstructions?, *Climate Dyn.*, 24, 577–590, 2005. 50
- Joussaume, S. and Taylor, K.: The Paleoclimate Modeling Intercomparison Project, in: *Paleoclimate Modeling Intercomparison Project (PMIP)*, edited by Braconnot, P., no. 1007 in WMO/TD, pp. 9–24, WMO, Geneva (CH), (WCRP-111), 2000. 38
- Kageyama, M. and Valdes, P. J.: Impacts of the North American ice-sheet orography on the Last Glacial Maximum eddies and snowfall, *Geophys. Res. Lett.*, 27, 1515–1518, 2000. 46
- Kageyama, M., Peyron, O., Pinot, S., Tarasov, P., Guiot, J., Joussaume, S., and Ramstein, G.: The Last Glacial Maximum climate over Europe and western Siberia: a PMIP comparison between models and data, *Climate Dyn.*, 17, 23–43, 2001. 48, 49, 50, 52
- Kageyama, M., Lané, A., Abe-Ouchi, A., Braconnot, P., Cortijo, E., Crucifix, M., Vernal, A. D., Guiot, J., Hewitt, C. D., Kitoh, A., Marti, M. K. O., Ohgaito, R., Otto-Bliesner, B., Peltier, W. R., Rosell-Melé, A., Vettoretti, G., Weber, S. L., Yu, Y., and MARGO Project Members: Last Glacial Maximum temperatures over the North Atlantic, Europe and western Siberia: a comparison between PMIP models, MARGO sea-surface temperatures and pollen-based reconstructions, *Quat. Sci. Rev.*, 25, 2082–2102, 2006. 49, 52
- Kaplan, J. O.: Geophysical application of vegetation modeling, PhD Thesis, Lund University, Lund, 2001. 48
- Kubatzki, C. and Claussen, M.: Simulation of the global biogeophysical interactions during the Last Glacial Maximum, *Climate Dyn.*, 14, 461–471, 1998. 46, 47
- Kucera, M., Rosell-Melé, A., Schneider, R., Waelbroeck, C., and Weinelt, M.: Multiproxy approach for the reconstruction of the glacial ocean surface (MARGO), *Quat. Sci. Rev.*, 24, 813–819, 2005. 31
- Laurent, J.-M., François, L., Bar-Hen, A., Bel, L., and Cheddadi, R.: European Bioclimatic Affinity Groups: data-model comparisons, *Global Planet. Change*, 61, 28–40, 2008. 32
- Levis, S., Foley, J. A., and Pollard, D.: CO<sub>2</sub>, climate and vegetation feedbacks at the Last Glacial Maximum, *J. Geophys. Res.*, 104, 31 191–31 198, 1999. 46, 47
- Manabe, S. and Broccoli, A. J.: The influence of Continental Ice Sheets on the Climate of an Ice Age, *J. Geophys. Res.*, 90, 2167–2190, 1985. 46
- Mark, B., Harrison, S., Spessa, A., New, M., Evans, D., and Helmens, K.: Tropical snowline changes at the Last Glacial Maximum: A global assessment, *Quaternary International*, 138–139, 168–201, 2005. 50
- Nemry, B., François, L. M., Warnant, P., Robinet, F., and Gérard, J.-C.: The seasonality of

---

**Land surface properties and CO<sub>2</sub> – effects on LGM climate**

---

A.-J. Henrot et al.

---

[Title Page](#)[Abstract](#)[Introduction](#)[Conclusions](#)[References](#)[Tables](#)[Figures](#)[⏪](#)[⏩](#)[◀](#)[▶](#)[Back](#)[Close](#)[Full Screen / Esc](#)[Printer-friendly Version](#)[Interactive Discussion](#)

---

**Land surface  
properties and CO<sub>2</sub> –  
effects on LGM  
climate**

---

A.-J. Henrot et al.

[Title Page](#)[Abstract](#)[Introduction](#)[Conclusions](#)[References](#)[Tables](#)[Figures](#)[⏪](#)[⏩](#)[◀](#)[▶](#)[Back](#)[Close](#)[Full Screen / Esc](#)[Printer-friendly Version](#)[Interactive Discussion](#)

the CO<sub>2</sub> exchange between the atmosphere and the land biosphere: A study with a global mechanistic vegetation model, *J. Geophys. Res.*, 101, 7111–7125, 1996. 32

Otto, D., Rasse, D., Kaplan, J., Warnant, P., and François, L.: Biospheric carbon stocks reconstructed at the Last Glacial Maximum: comparison between general circulation models using prescribed and computed sea surface temperatures, *Global Planet. Change*, 33, 117–138, 2002. 33, 35

Pedersen, T. F., François, R., François, L., Alverson, K., and McManus, J.: The Late Quaternary History of Biogeochemical Cycling of Carbon, in: *Paleoclimate, Global Change and the Future*, edited by: Alverson, K. D., Bradley, R. S., and Pedersen, T. F., Springer-Verlag, Berlin, Germany, chap. 4, 63–78, 2003. 35

Peltier, W. R.: Global glacial isostasy and the surface of the ice-age Earth: the ICE-5G (VM2) Model and GRACE, *Annu. Rev. Earth Planet. Sci.*, 32, 49–111, 2004. 34

Petit, J.-R., Jouzel, J., Raynaud, D., Barkov, N. I., Barnola, J.-M., Basile, I., Bender, M., Chappellaz, J., Davis, M., Delaygue, G., Delmotte, M., Kotlyakov, V. M., Legrand, M., Lipenkov, V. Y., Lorius, C., Pépin, L., Ritz, C., Saltzman, E., and Stievenard, M.: Climate and atmospheric history of the past 420,000 years from the Vostok ice core, Antarctica, *Nature*, 399, 429–436, 1999. 34

Pickett, E., Harrison, S. P., Hope, G., Harle, K., Dodson, J. R., Kershaw, A. P., Prentice, I. C., Backhouse, J., Colhoun, E. A., D'Costa, D., Flenley, J., Grindrod, J., Haberle, S., Hassell, C., Kenyon, C., Macphail, M., Martin, H., Martin, A. H., McKenzie, M., Newsome, J. C., Penny, D., Powell, J., Raine, I., Southern, W., Sutra, J., Thomas, I., van der Kaars, S., and Ward, J.: Pollen-based reconstructions of biome distributions for Australia, South East Asia and the Pacific (SEAPAC region) at 0, 6000 and 18,000 14C yr B.P., *J. Biogeogr.*, 31, 1381–1444, 2004. 35

Prentice, I. C., Jolly, D., and BIOME 6000 Participants: Mid-Holocene and glacial-maximum vegetation geography of the northern continents and Africa, *J. Biogeogr.*, 27(3), 507–519, 2000. 35, 48, 51

Ramstein, G., Kageyama, M., Guiot, J., Wu, H., Hély, C., Krinner, G., and Brewer, S.: How cold was Europe at the Last Glacial Maximum? A synthesis of the progress achieved since the first PMIP model-data comparison, *Clim. Past*, 3, 331–339, 2007, <http://www.clim-past.net/3/331/2007/>. 48

Rind, D.: Components of the Ice Age Circulation, *J. Geophys. Res.*, 92, 4241–4281, 1987. 46

Roeckner, E., Arpe, K., Bengtsson, L., Christoph, M., Claussen, M., Dumenil, L., Esch, M.,

---

**Land surface  
properties and CO<sub>2</sub> –  
effects on LGM  
climate**A.-J. Henrot et al.

---

- Giorgetta, M., and Schlese, U.: The Atmospheric General Circulation Model ECHAM4: model description and simulation of present day climate, Tech. Rep. 218, Max-Planck-Institute for Meteorology, Hamburg, 1996. 35
- Schneider von Deimling, T., Ganopolski, A., and Held, H.: How cold was the Last Glacial Maximum?, *Geophys. Res. Lett.*, 33, L14 709, 2006. 31, 45
- Stein, U. and Alpert, P.: Factor Separation in Numerical Simulations, *J. Atmos. Sci.*, 50(14), 2107–2115, 1993. 31, 33, 51
- Warnant, P., François, L. M., Strivay, D., and Gérard, J.-C.: CARAIB: A global model of terrestrial biological productivity, *Global Biogeochem. Cycles*, 8, 255–270, 1994. 32
- Williams, J. W., III, T. W., Richard, P. H., and Newby, P.: Late Quaternary biomes of Canada and the eastern United States, *J. Biogeogr.*, 27, 585–607, 2000. 36
- Wu, H., Guiot, J., Brewer, S., and Guo, Z.: Climatic changes in Eurasia and Africa at the last glacial maximum and mid-Holocene: reconstruction from pollen data using inverse vegetation modelling, *Climate Dyn.*, 29, 211–229, 2007. 32, 48, 49, 52
- Wyputta, U. and McAveney, B. J.: Influence of vegetation changes during the Last Glacial Maximum using the BMRC atmospheric general circulation model, *Climate Dyn.*, 17, 923–932, 2001. 46, 52
- Yanase, W. and Abe Ouchi, A.: The LGM surface climate and atmospheric circulation over East Asia and the North Pacific in the PMIP2 coupled model simulations, *Clim. Past*, 3, 439–451, 2007, <http://www.clim-past.net/3/439/2007/>. 47

[Title Page](#)[Abstract](#)[Introduction](#)[Conclusions](#)[References](#)[Tables](#)[Figures](#)[⏪](#)[⏩](#)[◀](#)[▶](#)[Back](#)[Close](#)[Full Screen / Esc](#)[Printer-friendly Version](#)[Interactive Discussion](#)

## Land surface properties and CO<sub>2</sub> – effects on LGM climate

A.-J. Henrot et al.

**Table 1.** Characteristics of the 16 simulation experiments. – refers to control values and + refers to LGM values. Each of the 4 columns corresponds to one of the four factors analysed: atmospheric CO<sub>2</sub>, ice cover, orography and surface albedo.

Acronym	CO <sub>2</sub>	ICE	ORO	VEG
CTRL	–	–	–	–
C	+	–	–	–
I	–	+	–	–
O	–	–	+	–
V	–	–	–	+
CI	+	+	–	–
CO	+	–	+	–
CV	+	–	–	+
IO	–	+	+	–
IV	–	+	–	+
OV	–	–	+	+
CIO	+	+	+	–
CIV	+	+	–	+
COV	+	–	+	+
IOV	–	+	+	+
LGM	+	+	+	+

[Title Page](#)
[Abstract](#)
[Introduction](#)
[Conclusions](#)
[References](#)
[Tables](#)
[Figures](#)




[Back](#)
[Close](#)
[Full Screen / Esc](#)
[Printer-friendly Version](#)
[Interactive Discussion](#)

**Land surface  
properties and CO<sub>2</sub> –  
effects on LGM  
climate**

A.-J. Henrot et al.

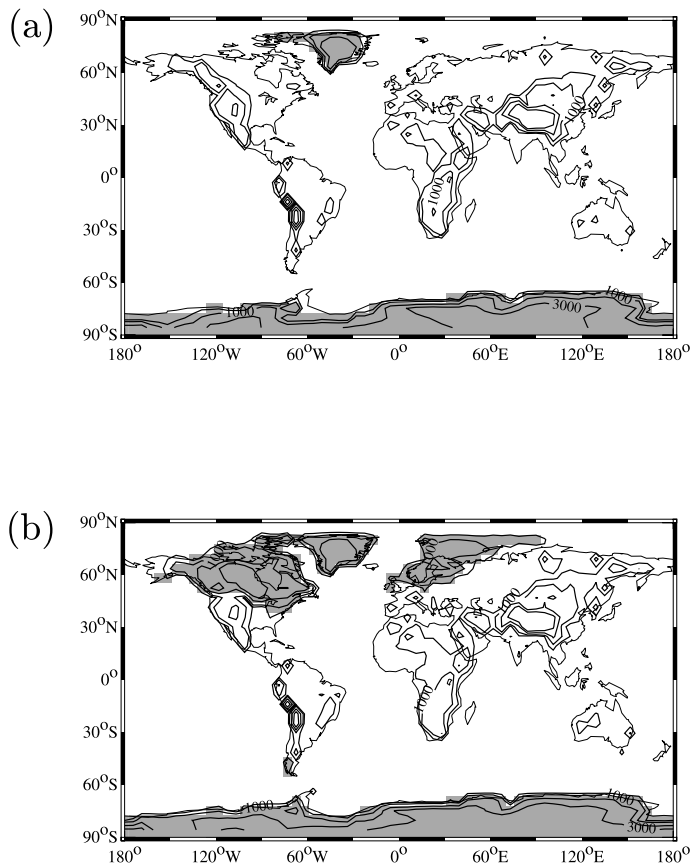


**Fig. 1.** Glacier mask and orography used as boundary conditions for **(a)** the control state and the experiments without ice cover and orography changes, and **(b)** the LGM state and the experiments with ice cover or orography changes.

[Title Page](#)[Abstract](#)[Introduction](#)[Conclusions](#)[References](#)[Tables](#)[Figures](#)[◀](#)[▶](#)[◀](#)[▶](#)[Back](#)[Close](#)[Full Screen / Esc](#)[Printer-friendly Version](#)[Interactive Discussion](#)

## Land surface properties and CO<sub>2</sub> – effects on LGM climate

A.-J. Henrot et al.

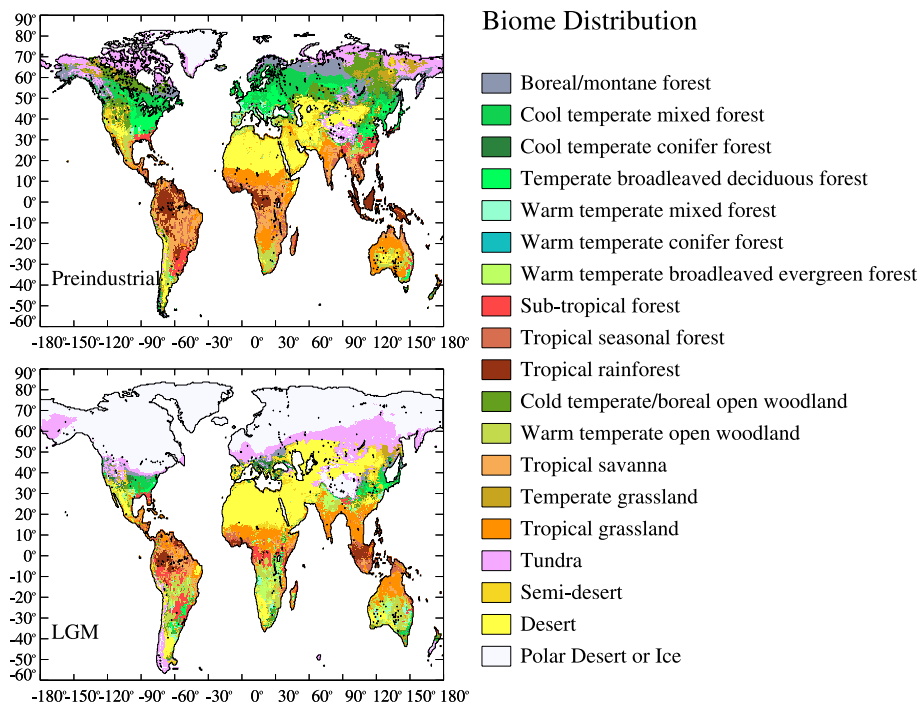


**Fig. 2.** Biome distributions from CARAIB preindustrial and LGM equilibrium runs.

Title Page

Abstract

Introduction

Conclusions

References

Tables

Figures

◀

▶

◀

▶

Back

Close

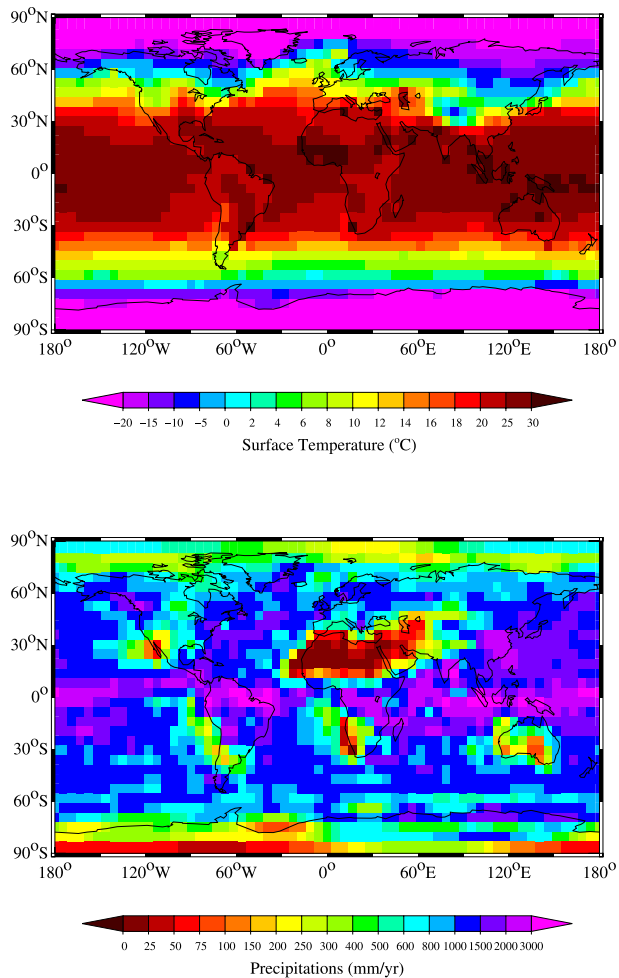
Full Screen / Esc

Printer-friendly Version

Interactive Discussion

**Land surface  
properties and CO<sub>2</sub> –  
effects on LGM  
climate**

A.-J. Henrot et al.

**Fig. 3.** Annual surface temperature and precipitation of the control experiment (CTRL).[Title Page](#)[Abstract](#)[Introduction](#)[Conclusions](#)[References](#)[Tables](#)[Figures](#)[◀](#)[▶](#)[◀](#)[▶](#)[Back](#)[Close](#)[Full Screen / Esc](#)[Printer-friendly Version](#)[Interactive Discussion](#)

## Land surface properties and CO<sub>2</sub> – effects on LGM climate

A.-J. Henrot et al.

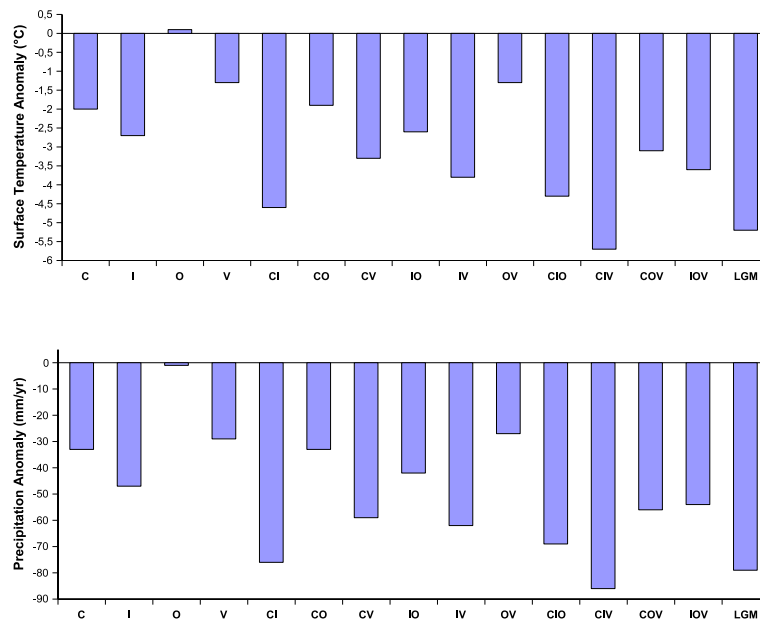


**Fig. 4.** Global surface temperature and precipitation anomalies (EXPERIMENT-CTRL). All results reported here are global means over the last 20 years of 50-year simulations, allowing 30 years for the model to equilibrate.

Title Page

Abstract

Introduction

Conclusions

References

Tables

Figures

⏪

⏩

◀

▶

Back

Close

Full Screen / Esc

Printer-friendly Version

Interactive Discussion

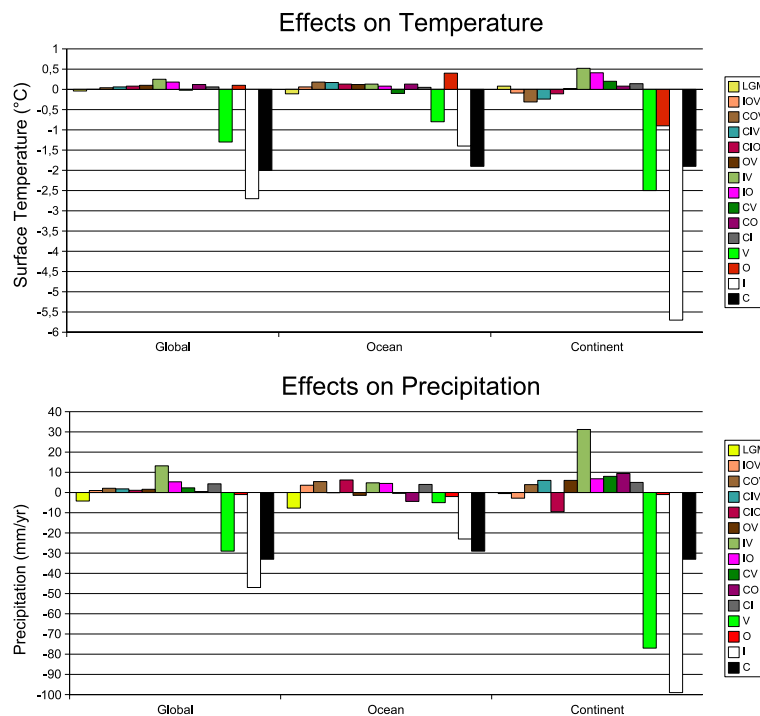


**Fig. 5.** Comparison of the pure contributions with the effects of the interactions between the factors on the global, oceanic and continental annual surface temperature and precipitation. The C, I, O, V effects represent the pure contributions of each factor. The CI to LGM effects represent the contributions of the *interactions* among the corresponding factors, not the actual effects, which are shown on Fig. 4.

[Title Page](#)
[Abstract](#)
[Introduction](#)
[Conclusions](#)
[References](#)
[Tables](#)
[Figures](#)
[⏪](#)
[⏩](#)
[⏴](#)
[⏵](#)
[Back](#)
[Close](#)
[Full Screen / Esc](#)
[Printer-friendly Version](#)
[Interactive Discussion](#)

**Land surface  
properties and CO<sub>2</sub> –  
effects on LGM  
climate**

A.-J. Henrot et al.

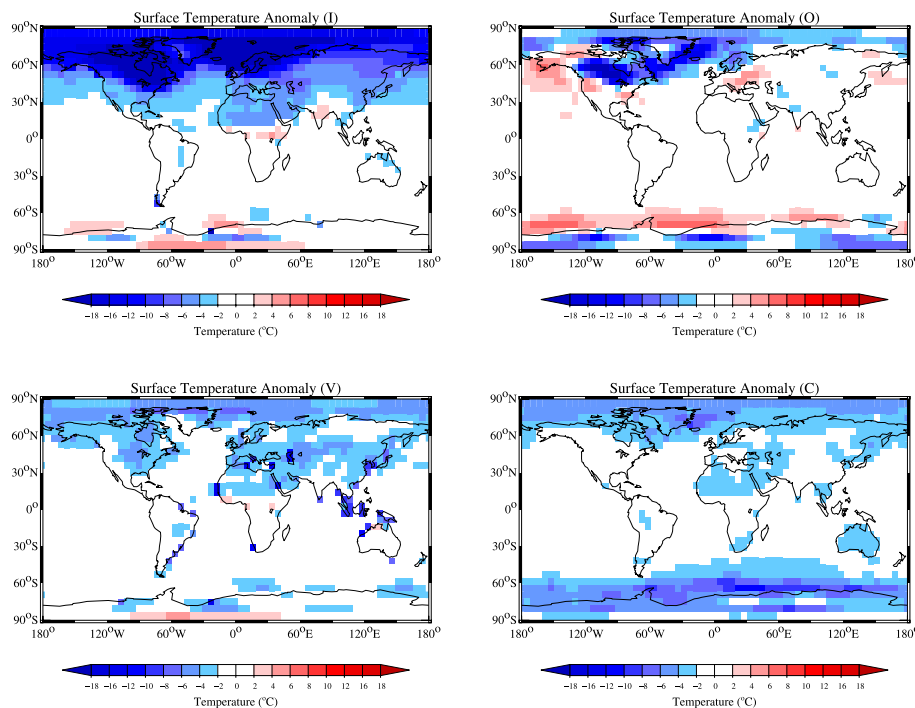


**Fig. 6.** Annual surface temperature anomalies (EXPERIMENT-CTRL) resulting from the experiments I, O, V and C.

[Title Page](#)[Abstract](#)[Introduction](#)[Conclusions](#)[References](#)[Tables](#)[Figures](#)[◀](#)[▶](#)[◀](#)[▶](#)[Back](#)[Close](#)[Full Screen / Esc](#)[Printer-friendly Version](#)[Interactive Discussion](#)

---

**Land surface  
properties and CO<sub>2</sub> –  
effects on LGM  
climate**A.-J. Henrot et al.

---

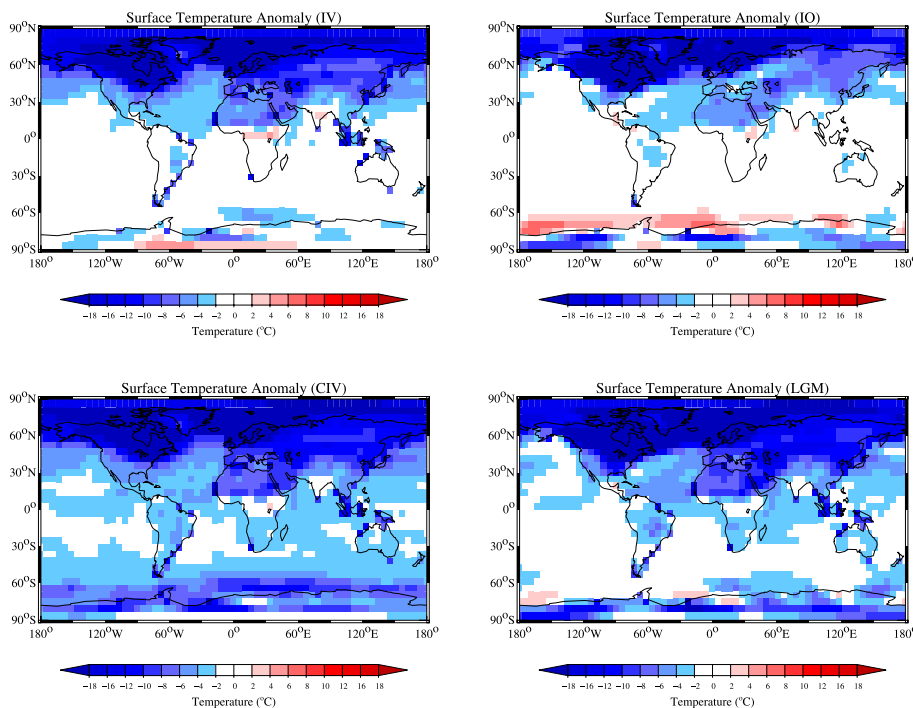


**Fig. 7.** Annual surface temperature anomalies (EXPERIMENT-CTRL) resulting from the experiments IV, IO, CIV and LGM.

[Title Page](#)[Abstract](#)[Introduction](#)[Conclusions](#)[References](#)[Tables](#)[Figures](#)[⏪](#)[⏩](#)[◀](#)[▶](#)[Back](#)[Close](#)[Full Screen / Esc](#)[Printer-friendly Version](#)[Interactive Discussion](#)

**Land surface  
properties and CO<sub>2</sub> –  
effects on LGM  
climate**

A.-J. Henrot et al.

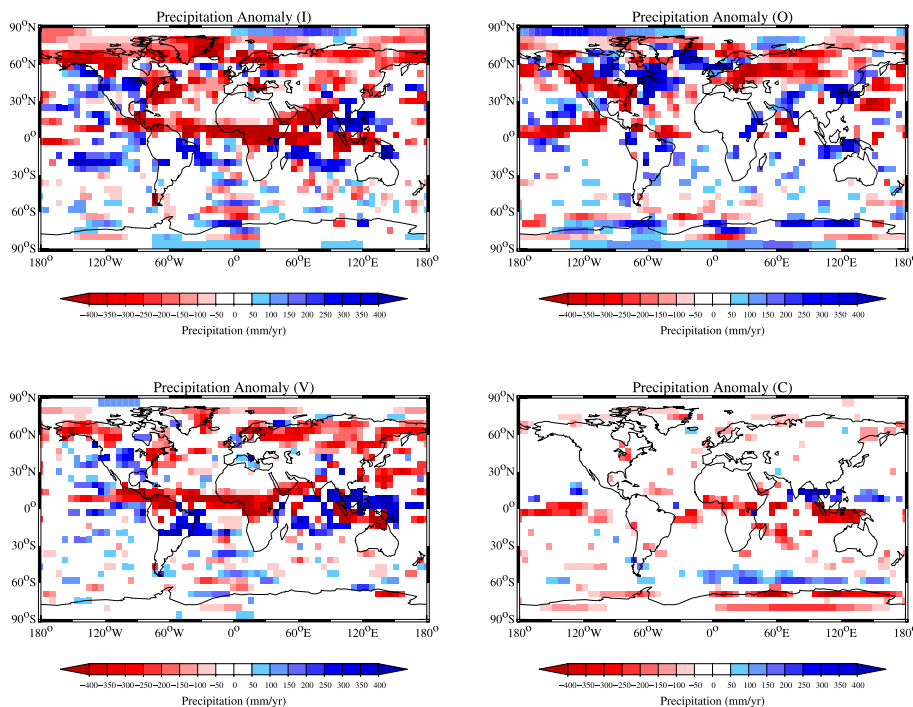


**Fig. 8.** Annual precipitation anomalies (EXPERIMENT-CTRL) resulting from the experiments I, O, V and C. Only the anomalies greater than one standard deviation for the long term annual mean over the last 20 years are shown.

[Title Page](#)[Abstract](#)[Introduction](#)[Conclusions](#)[References](#)[Tables](#)[Figures](#)[◀](#)[▶](#)[◀](#)[▶](#)[Back](#)[Close](#)[Full Screen / Esc](#)[Printer-friendly Version](#)[Interactive Discussion](#)

## Land surface properties and CO<sub>2</sub> – effects on LGM climate

A.-J. Henrot et al.

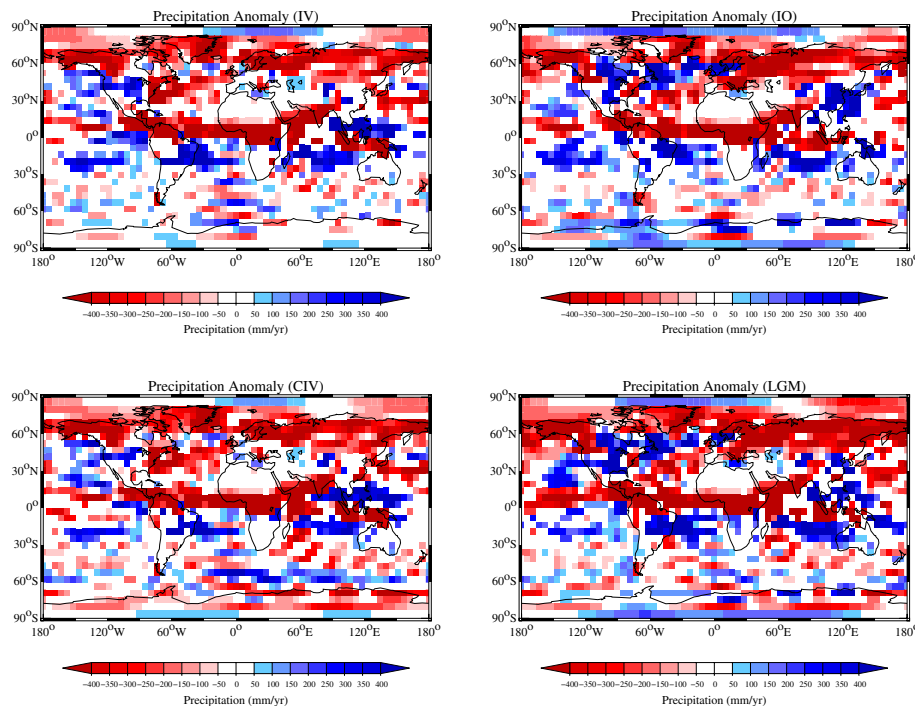


**Fig. 9.** Annual precipitation anomalies (EXPERIMENT-CTRL) resulting from the experiments IV, IO, CIV and LGM. Only the anomalies greater than one standard deviation for the long term annual mean over the last 20 years are shown.

Title Page

Abstract

Introduction

Conclusions

References

Tables

Figures

◀

▶

◀

▶

Back

Close

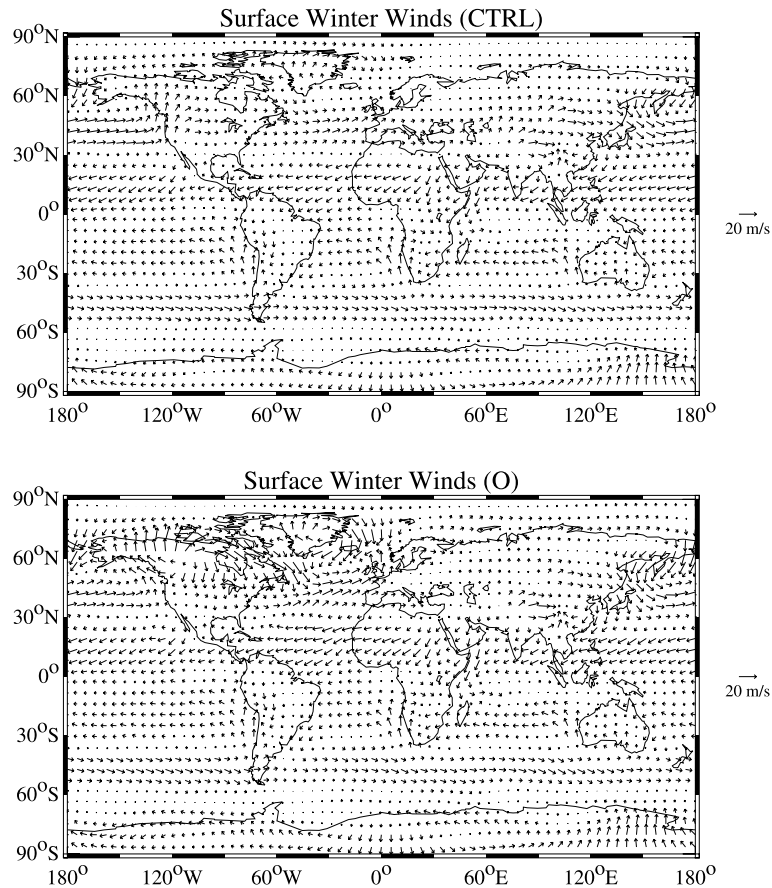
Full Screen / Esc

Printer-friendly Version

Interactive Discussion

**Land surface  
properties and CO<sub>2</sub> –  
effects on LGM  
climate**

A.-J. Henrot et al.

**Fig. 10.** Surface winter winds resulting from the experiments CTRL and O.[Title Page](#)[Abstract](#)[Introduction](#)[Conclusions](#)[References](#)[Tables](#)[Figures](#)[◀](#)[▶](#)[◀](#)[▶](#)[Back](#)[Close](#)[Full Screen / Esc](#)[Printer-friendly Version](#)[Interactive Discussion](#)

## Land surface properties and CO<sub>2</sub> – effects on LGM climate

A.-J. Henrot et al.

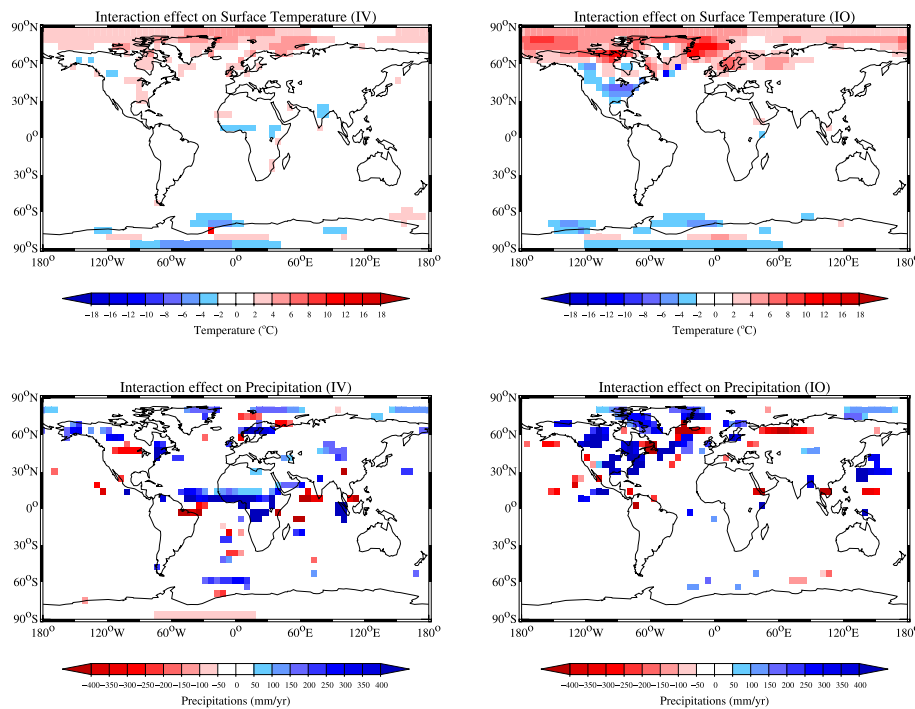


**Fig. 11.** Effects of the interactions IV and IO on surface temperature and precipitation.

Title Page

Abstract

Introduction

Conclusions

References

Tables

Figures

⏪

⏩

◀

▶

Back

Close

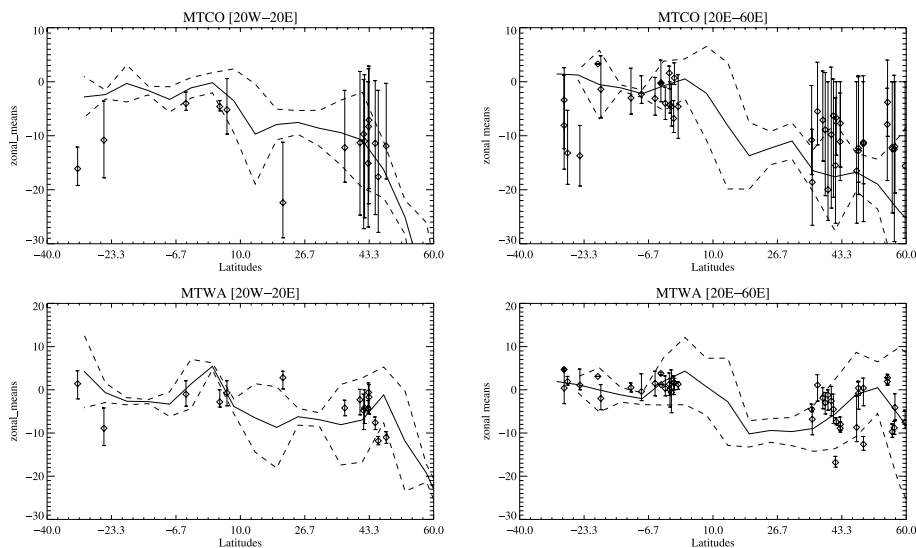
Full Screen / Esc

Printer-friendly Version

Interactive Discussion

**Land surface  
properties and CO<sub>2</sub> –  
effects on LGM  
climate**

A.-J. Henrot et al.

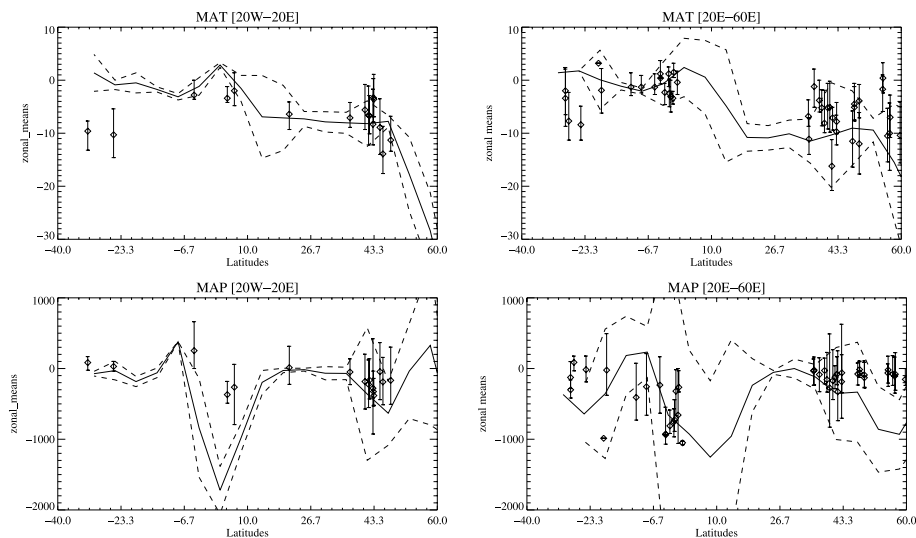


**Fig. 12.** Comparison between model results and data for the LGM-PRESENT anomalies in MTCO and MTWA and for the two sectors (20° W–20° E) and (20° E–60° E). The longitudinal averages over land points for the model and the data with confidence intervals are shown.

[Title Page](#)[Abstract](#)[Introduction](#)[Conclusions](#)[References](#)[Tables](#)[Figures](#)[◀](#)[▶](#)[◀](#)[▶](#)[Back](#)[Close](#)[Full Screen / Esc](#)[Printer-friendly Version](#)[Interactive Discussion](#)

**Land surface  
properties and CO<sub>2</sub> –  
effects on LGM  
climate**

A.-J. Henrot et al.

**Fig. 13.** Same as Fig. 12 for the MAT and MAP anomalies.[Title Page](#)[Abstract](#)[Introduction](#)[Conclusions](#)[References](#)[Tables](#)[Figures](#)[◀](#)[▶](#)[◀](#)[▶](#)[Back](#)[Close](#)[Full Screen / Esc](#)[Printer-friendly Version](#)[Interactive Discussion](#)